Fueling characteristics of supersonic gas puffing applied to large high-temperature plasma in LHD

A. Murakami[1, 2], J. Miyazawa[3], C. Suzuki[3], I. Yamada[3], T. Morisaki[3], R. Sakamoto[3], H. Yamada[3] and LHD Experiment Group

[1)]The Graduate University for Advanced Studies (SOKENDAI), Toki 509-5292, Japan

[2)]Research Fellow of the Japan Society for the Promotion of Science

[3)]National Institute for Fusion Science (NIFS), Toki 509-5292, Japan

Introduction

Development of fueling methods is a critical issue for realization of fusion DEMO reactor. Recently, supersonic molecular beam injection (SMBI) in HL-2A [1,2], supersonic pulsed gas injection (SPGI) in Tore Supra tokamak [3] and supersonic gas injector (SGI) in NSTX [4] have been developed as new fueling methods. These have also been applied to ASDEX-U [5], JT-60U [6] and Heliotron J [7] to understand the fueling characteristics. For example, a fueling efficiency of 30 ~ 60 % has been achieved by SPGI in the Tore Supra tokamak [3]. Supersonic gas puffing (SSGP) also has been applied to large high-temperature plasma and its fueling characteristics have been investigated in the Large Helical Devise (LHD). The SSGP injection method, where a high-pressure hydrogen gas is ejected through the fast solenoid valve equipped with Laval nozzle, has been developed as a new fueling method for LHD [8, 9]. In this paper, the fueling characteristics of SSGP applied to large high-temperature plasma are discussed based on the analysis of electron density profile data.

Experimental Set-up

Figure 1 shows the supersonic gas puffing (SSGP) system in LHD. The SSGP system has been installed on the lower port of LHD. The distance from valves to the plasma is about 4 m. The solenoid valves used in the SSGP system are characterised by the shorter response time of < 1 ms and the higher working pressure of < 8 MPa than those of piezoelectric valves used in ordinary gas puff system in LHD. Three solenoid valves are equipped with different Laval nozzles of 0.1, 0.3 and 0.6 mm throat diameter, respectively (Fig. 2). These Laval nozzles were designed to generate gas flow of Mach number 8. The hydrogen gas flow speed measured in the test-stand is, however, ~ 1 km/s, which corresponds to the hydrogen sound speed at the room temperature. The divergence of supersonic gas flow has been decreased after installation of these Laval nozzles

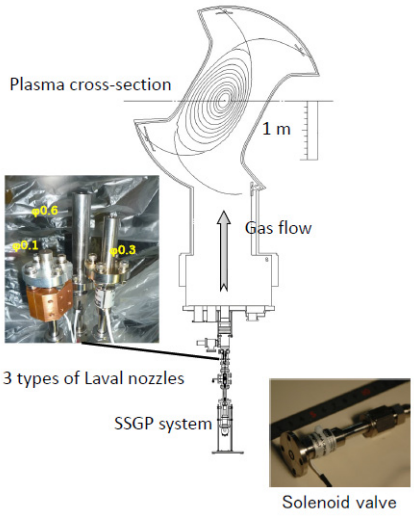

Fig. 1 SSGP system on LHD. The distance from valves to plasma is about 4 m. Three types of Laval nozzles are installed on SSGP system.

from 22.5° to ~10°. By selecting the nozzles and the backing pressure, the flow rate of SSGP can be adjusted from 1 to 1000 Pa*m^3/s. Figure 2 shows the measured flow rate table and cross sections of three types of Laval nozzles. When the backing pressure is 5.0 MPa, which is the pressure of SSGP in a series of experiments discussed hereinafter, the electron flux, Γ_{SSGP}, of Laval nozzles of 0.1, 0.3 and 0.6 mm throat diameter are 3.9, 9.3 and 27.2 × 10^{22} particles/s, respectively. In order to investigate the fueling characteristics, density ramp-up experiments have been carried out using these Laval nozzles.

	Φ0.1 Laval nozzle	Φ0.3 Laval nozzle	Φ0.6 Laval nozzle
Throat diameter [mm]	0.1	0.3	0.6
Flux [Pa*m³/s] @H_2, 1.0 MPa	17	41	120
Flux [Pa*m³/s] @H_2, 5.0 MPa	79	190	556
particle flux Γ_{SSGP} [10^{22} particles / s] @H_2, 5.0 MPa	3.9	9.3	27.2

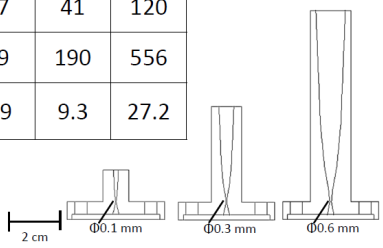

Fig. 2 Flow rate table of SSGP and cross sections of three types of Laval nozzles. The flow rate of ϕ0.3 Laval nozzle is about three times smaller than that of ϕ0.6 Laval nozzle and about three times larger than that of that of ϕ0.1 Laval nozzle.

Results

Figure 3 shows typical temporal evolutions of the line-averaged electron density $\overline{n_e}$ and radial density profiles fueled by the three Laval nozzles. In a series of experiments, the magnetic field strength on the magnetic axis was fixed to 1.5 T. The major radius and the minor radius of the plasma were 3.6 m and 0.6 m, respectively. The line-averaged electron density was increased by 1 × 10^{19} m^{-3} (ϕ0.1), 2.5 × 10^{19} m^{-3} (ϕ0.3), and 3.5 × 10^{19} m^{-3} (ϕ0.6) after SSGP, where SSGP was injected at t = 3.765 s with a pulse length of 200 ms (ϕ0.1), 50 ms (ϕ0.3) and 20 ms (ϕ0.6), respectively (see Figs. 3 (a), (c), and (e)). The hatched region shown in Figs. 3 (a), (c), and (e) denotes the valve open time. Figures 3 (b), (d), and (f) show radial profiles of electron density before (t = 3.766 s) and during/after (t = 3.800 s) SSGP, measured by a YAG Thomson scattering system. It should be noted that the line-averaged density kept increasing after SSGP, especially in Figs. 3 (c) and (e). Figures 3 (d) and (f) show that large increase in the electron density profile was observed at ρ = 1.02, where ρ is the normalized minor radius. In the case of ϕ0.6 Laval nozzle, a hollow density profile with steep inward gradient was formed after SSGP, as shown in Fig. 3 (f). According to these observation,

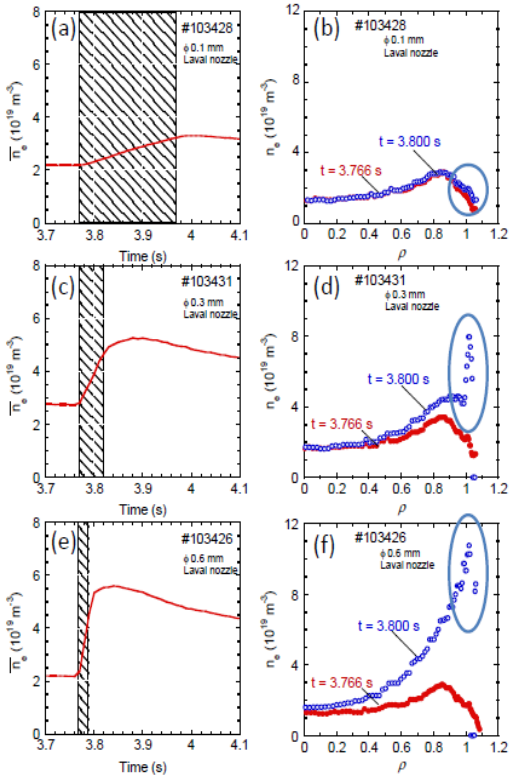

Fig. 3 Typical temporal evolutions of the line-averaged electron density n_e (a), (c), and (e) and radial electron density profiles (b), (d), and (f) of three types of Laval nozzles. In radial profiles, closed and open symbols denote before and after SSGP, respectively. The hatched region in (a), (c), and (e) indicates the valve open time.

SSGP deposits the particles in the plasma edge region ($\rho \sim 1.02$), which is the region outside last closed flux surface (LCFS), independent of the type of Laval nozzle. Rapid increase of line-averaged density in the cases of ϕ0.3 and ϕ0.6 Laval nozzle after SSGP was caused by the edge density increase.

Fueling efficiency of the SSGP in the case of ϕ0.3 Laval nozzle has been investigated by the density ramp-up experiments. The total electron inventory,

$$N_e(t) = \int_0^{1.0} n_e(\rho)\frac{dV}{d\rho}\,d\rho, \qquad (1)$$

was estimated from radial electron density profiles measured by the Thomson scattering system. Fueling efficiency was estimated from the time derivative of N_e and the SSGP flow rate ($\Gamma_{SSGP} = 9.3\times10^{22}$ particles / s in the case of ϕ0.3 Laval nozzle) as follows,

$$\eta = \frac{dN_e/dt}{\Gamma_{SSGP}}\times 100. \qquad (2)$$

Figure 4 (a) shows the fueling efficiency as a function of the electron line-averaged density before SSGP. Fueling efficiency decreases as the electron density before SSGP increases. Figure 5 shows two radial electron density profiles in the cases of high (a) and low (b) fueling efficiency, where SSGP was injected at t = 3.765 s and t = 3.965 s with same pulse length of 50 ms. In the case of high efficiency, electron density before SSGP (t = 3.766 s) is low and the electron density was increased at ρ = 0.40 - 1.00 region during SSGP (t = 3.800 s). On the other hand, the edge electron density before SSGP was already high in the case of low efficiency. The electron density increase was limited to the edge region of ρ > 0.80. If we assume that the amounts of electron density rise at $\rho = 1.02$ were same for the cases of high and low efficiency, the inward gradient of density profile just after SSGP should depend on the edge density at $\rho \sim 1.00$, n_{e_edge}, before SSGP. In other words, the inward gradient of density profile became steep just after SSGP when the edge density was low ($n_{e\_edge} \sim 1 \times 10^{19}$ m^{-3}). Meanwhile, the inward gradient was mild when the edge density was high ($n_{e\_edge} \sim 3 \times 10^{19}$ m^{-3}). The inward gradient of density profiles transports particles from edge to core region through diffusion process. Figure 4 (b) shows the fueling efficiency as a function of the edge electron density, n_{e_edge}. Fueling efficiency indicates the property of strong dependence on the edge

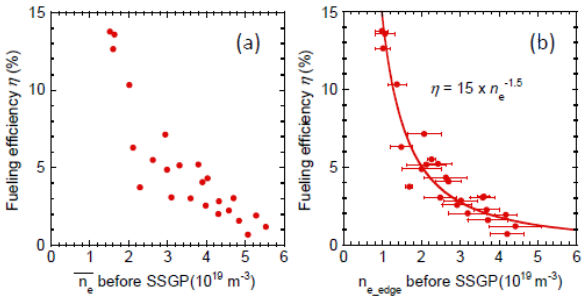

Fig. 4 (a) Fueling efficiency in the case of ϕ0.3 Laval nozzle as a function of the electron line-averaged density before SSGP. (b) Fueling efficiency indicates the exponential dependence on the edge electron density ($\rho \sim$ 1.0) before SSGP.

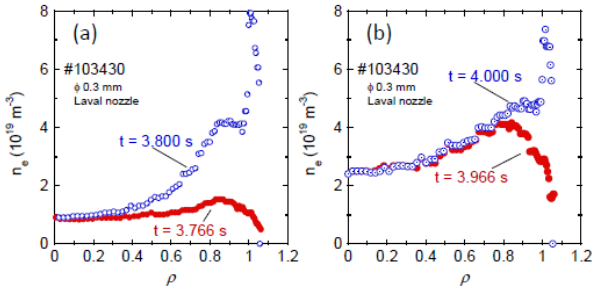

Fig. 5 Radial electron density profiles in the cases of (a) high and (b) low fueling efficiency. Closed and open symbols denote before and after SSGP, respectively.

electron density before SSGP. In order to obtain high efficiency, a steep inward gradient should be maintained. This can be realized when the edge electron density before SSGP is low enough, or the amount of density increase is much higher than the edge electron density before SSGP.

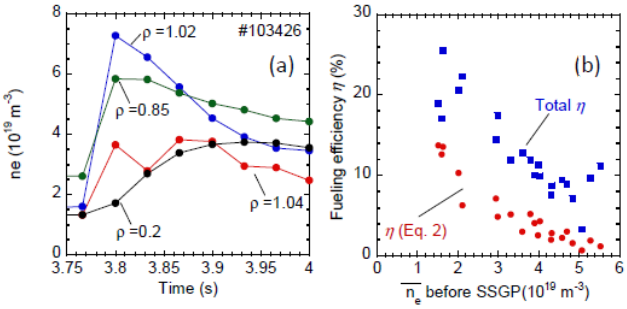

Fig. 6 Temporal evolutions of (a) the electron density at different normalized minor radius and (b) total fueling efficiency as a function of line-averaged electron density before SSGP.

Figures 3 (c) and (e) show that the line-averaged density kept increasing after SSGP. In density increasing process after SSGP, core density is increased by the diffusion from the edge region. Figure 6 (a) shows the temporal evolutions of the electron density at different normalized minor radius in the same discharge as shown in Figs. 3 (c) and (f). Slow increase of core density ($\rho = 0.20$) indicates the diffusion process of electron density from the edge region to the core region. The electron density increase including this diffusion process after SSGP should be considered to evaluate the fueling efficiency of SSGP. Estimation of the fueling efficiency with Eq. (2) is limited to during SSGP and does not include this diffusion process after SSGP. In this study, the total fueling efficiency is defined as a ratio of increase in the total electron number including the density increase after SSGP to the injected electron number by SSGP. This definition is similar to those used in Refs. 2-3. Figure 6 (b) shows the total fueling efficiency as a function of the line-averaged density before SSGP. The total fueling efficiency is two times higher than the fueling efficiency defined by Eq. (2) (η_{total} = 10 ~ 30 %).

Summary

Fueling characteristics of SSGP have been investigated in LHD. Radial position of increase in the electron density profile is outside of the LCFS (ρ = 1.02). Fueling efficiency strongly depends on the edge electron density (ρ ~ 1.00) before SSGP. After SSGP, core density increases due to the particle diffusion from the edge to the core. The total fueling efficiency including the density increase after SSGP is 10 ~ 30 %.

Acknowledgement

The authors would like to thank all of the members of LHD Experiment Group. This work has been financially supported by the Ministry of Education, Sports, Culture, Science and Technology, Grants-in-Aid for Scientific Research (S) 20226018 and NIFS09ULFF006.

References

[1] L. Yao et al., Nucl. Fusion **47**, 1399 (2007)
[2] C.Y. Chen et al., J. Plasma Fusion Res. SERIES **9**, 37 (2010)
[3] B. Pegourie et al., J. Nucl. Materials **313**, 539 (2003)
[4] V.A.Soukhanovskii et al., Rev. Sci. Instrum. **75**, 4320 (2004)
[5] P. T. Lang et al., Plasma phys. Control. Fusion **47** 1495 (2005)
[6] H. Takenaga et al., Nucl. Fusion **50** 115003 (2010)
[7] T. Mizuuchi et al., Cotrib. Plasma Phys. **50** N0.6-7, 639 (2010)
[8] A. Murakami et al., Plasma Fusion Res. **5**, S1032 (2010)
[9] A. Murakami et al., J. Plasma Fusion Res. SERIES **9**, 979 (2010)